New Phytologist

Research

Mosaics often outperform pyramids: insights from a model comparing strategies for the deployment of plant resistance genes against viruses in agricultural landscapes

Ramses Djidjou-Demasse[1], Benoît Moury[2] and Frédéric Fabre[1]

[1]UMR 1065, INRA, Villenave d'Ornon F-33882, France; [2]UR 407, Pathologie Végétale, INRA, Montfavet F-84140, France

Author for correspondence:
Frédéric Fabre
Tel: +33 557 122 642
Email: frederic.fabre@inra.fr

Received: *9 February 2017*
Accepted: *13 June 2017*

New Phytologist (2017) **216:** 239–253
doi: 10.1111/nph.14701

Key words: durable disease resistance, landscape epidemiology, major resistance gene, mosaic of plant resistance, pyramids of plant resistance, regional deployment strategy.

Summary

- The breakdown of plant virus resistance genes is a major issue in agriculture. We investigated whether a set of resistance genes would last longer when stacked into a single plant cultivar (pyramiding) or when deployed individually in regional mosaics (mosaic strategy).
- We modeled the genetic and epidemiological processes shaping the demogenetic dynamics of viruses under a multilocus gene-for-gene system, from the plant to landscape scales. The landscape consisted of many fields, was subject to seasonality, and of a reservoir hosting viruses year-round.
- Strategy performance depended principally on the fitness costs of adaptive mutations, epidemic intensity before resistance deployment and landscape connectivity. Mosaics were at least as good as pyramiding strategies in most production situations tested. Pyramiding strategies performed better only with slowly changing virus reservoir dynamics. Mosaics are more versatile than pyramiding strategies, and we found that deploying a mosaic of three to five resistance genes generally provided effective disease control, unless the epidemics were driven mostly by within-field infections.
- We considered the epidemiological and evolutionary mechanisms underlying the greater versatility of mosaics in our case study, with a view to providing breeders and growers with guidance as to the most appropriate deployment strategy.

Introduction

In addition to their impact on ecological dynamics, humans greatly influence the evolutionary trajectories of many species worldwide. This influence, which has been documented for many species, including pests and parasites, results mostly from the intensification of agriculture and medicine (Palumbi, 2001). The evolution of resistance to antibiotics in disease-causing bacteria is a textbook example of microbial adaptations that have become a major issue for public health (Palumbi, 2001). Similarly, the evolution of resistance to pesticides (insecticides, fungicides or herbicides) is a major issue in agriculture (REX Consortium, 2013). The breakdown of resistance genes introduced into crop varieties by plant breeders, particularly major resistance genes (*R* gene) conforming to the gene-for-gene (GFG) paradigm (Flor, 1971), is also a major problem. *R* genes often remain effective for only a few cropping seasons, whether they confer protection against fungi and bacteria (McDonald & Linde, 2002), or against viruses (García-Arenal & McDonald, 2003), as a result of the rapid counteradaptation of microbes.

The mechanisms underlying the adaptation of pathogen populations to xenobiotics and to plant *R* genes are basically the same: in both cases, pathogen fitness is reduced, and the pathogen evolves in response to this selection pressure. If the control method is applied to a large proportion of the population and is sustained over time, strong directional selection occurs, favoring the rapid adaptation of the pathogen (Palumbi, 2001; REX Consortium, 2013). This development of resistance initially led to the development of a 'responsive alternation' strategy, in which a molecule is repeatedly used on the whole population until adapted pathogens emerged, at which point a second molecule is introduced, and so on (REX Consortium, 2013). In plant pathology, the strong directional selection regimes resulting from such approaches have led to 'boom-and-bust' cycles. In this vicious circle, a new cultivar with a single *R* gene is widely adopted by farmers because it is effective against a large fraction of the pathogen population (the 'boom'). The pathogen then adapts, leading to the breakdown of resistance and withdrawal of the cultivar (the 'bust'). Such 'boom-and-bust' cycles are typical examples of anthropogenic evolution due to directional selection on a pathogen population when cultivars carrying a single *R* gene are widely cultivated over large geographic area dominated by monocultures of the crop concerned (McDonald & Linde, 2002; Zhan *et al.*, 2015).

Basic evolutionary mechanisms can be recruited to slow the pace of pathogen adaptation. There are two broad types of

strategy available for achieving this end: mosaic/periodic strategies and pyramiding. Mosaic strategies are based on a spatial pattern of application of at least two pesticides or drugs, whereas periodic strategies involve temporal patterns of application of at least two pesticides or drugs. For two *R* genes (R_1 and R_2) deployed in an agricultural landscape, the simplest mosaic strategy consists of the repeated planting, over cropping seasons, of half the field with a cultivar bearing R_1 and the other half with a cultivar bearing R_2. Mosaics mobilize evolutionary mechanisms, as they impose disruptive selection regimes on pathogen populations, with the selection environment designed to favor different pathogen genotypes at different locations within the landscape (McDonald & Linde, 2002; Zhan *et al.*, 2015). Mosaics also mobilize epidemiological mechanisms of which the well-known dilution effect (i.e. the reduction of infection efficiency by an increase in the distance between plants of the same genotype (Plantegenest *et al.*, 2007), initially described for the use of genotype mixtures within fields; Wolfe, 1985; Mundt, 2002). Combination strategies involve the concomitant use of two or more pesticides or drugs over space and time. The combination of two or more resistance genes in a single plant, known as pyramiding, is common practice in plant breeding. In the simplest pyramid, two *R* genes are inserted into a single cultivar (which therefore bears both R_1 and R_2), which is then repeatedly planted throughout the field over cropping seasons. Pyramids combine selection pressures applied in the same place, at the same time. The main expected outcome is to decrease the probability that the pathogen crossed the mutational pathway conferring adaption to each *R* gene (Mundt, 1990, 1991; McDonald & Linde, 2002).

Many theoretical studies have considered the best ways to make strategic use of xenobiotics to delay or prevent adaptation in a population of pests or pathogens (REX Consortium, 2013), but only a few have compared such strategies for the management of *R* genes (REX Consortium, 2016). As pointed out by Burdon *et al.* (2014), there have been very few theoretical assessments of the most effective strategies for resistance deployment. Zhan *et al.* (2015) also highlighted the lack of theoretical studies for the design of sustainable disease management strategies combining *R*-gene rotation 'with other deployment strategies such as pyramiding, regional gene deployment, and mixtures'.

We propose here a model coupling epidemiology and population genetics for studies of the best ways of associating susceptible and resistant cultivars in strategies for controlling epidemics over several seasons at the landscape scale. This model extends that of Fabre *et al.* (2012, 2015) involving a single-locus diallelic GFG system (i.e. only two pathogen variants and two plant genotypes were considered) into a multilocus GFG system. This new model can handle matrices of interaction between more than two pathogen variants and resistant cultivars. As such, it can provide a general comparison of a set of mosaic and pyramiding strategies, ranging from the simplest predefined strategies to more complex strategies optimized over space and time (Table 1).

Description

Model overview

The model describes plant epidemics during a succession of cropping seasons, for a haploid multilocus di-allelic GFG system. It can be applied to any plant pathogen for which within- and between-host dynamics are clearly separated, as is typically the case for viruses. The dynamics of epidemics are first modeled over a cropping season, in a landscape composed of many fields, each field being sown with one of (n_c+2) possible host plant genotypes: a susceptible cultivar (S), n_c cultivars with monogenic *R* ($R_1, R_2, \cdots, R_{n_c}$) and a cultivar pyramiding the n_c resistances ($R_{12\ldots n_c}$). These n_c+2 plant cultivars interact with n_c+2 pathogen pathotypes ($av, v_1, v_2, \cdots, v_{n_c}, v_{12\ldots n_c}$). Pathotypes are groups of pathogen genotypes with similar infectivity profiles. The *av* pathotype can infect only the *S* cultivar. Pathotypes v_i can infect only the monogenic cultivar with resistance gene R_i and the *S* cultivar. The $v_{12\ldots n_c}$ pathotype is the only pathotype able to infect all cultivars, including the $R_{12\ldots n_c}$ cultivar in which all the resistance genes are pyramided. Epidemics in successive cropping seasons are then coupled together through the interaction of the crop with a virus reservoir compartment, containing diverse wild plant species that may serve as hosts for the pathogen during the crop-free period and as a source of inoculum for the initiation of infections in the next cropping period. The reservoir is selectively neutral for the pathogen population. The main variables and

Table 1 Names and spatial/temporal characteristics of the deployment strategies compared

Strategy (short name)	Cultivar proportion	Space	Time	Proportion at year *i*	Proportion at year *i* + 1
Mosaic (MoS)	Fixed	Variable	Uniform	50% R_1–50% R_2	50% R_1–50% R_2
Pyramiding (PyS)	Fixed	Uniform	Uniform	Only R_{12}	Only R_{12}
Mosaic* (MoS*)	Optimal	Variable	Uniform	P_S, P_{R_1}, P_{R_2}	P_S, P_{R_1}, P_{R_2}
Var. mosaic* (vMoS*)	Optimal	Variable	Variable	$P_S^i, P_{R_1}^i, P_{R_2}^i$	$P_S^{i+1}, P_{R_1}^{i+1}, P_{R_2}^{i+1}$
Pyramiding* (PyS*)	Optimal	Variable	Uniform	$P_S, P_{R_{12}}$	$P_S, P_{R_{12}}$
Var. pyramiding* (vPyS*)	Optimal	Variable	Variable	$P_S^i, P_{R_{12}}^i$	$P_S^{i+1}, P_{R_{12}}^{i+1}$

These strategies are illustrated here with two resistance genes and the resulting four cultivars: a susceptible cultivar (*S*), two monogenic resistant cultivars R_1 and R_2, and a resistant cultivar pyramiding the two resistance genes (R_{12}). Simple strategies are the basic predefined strategies. Optimal strategies minimized the damage caused by the pathogen at the landscape scale. Optimal mosaic strategies best combined the proportions of *S* (P_S), R_1 (P_{R_1}) and R_2 (P_{R_2}) cultivars in the landscape, either using the same proportion each year (MoS*), or by varying these proportions from year to year (vMoS*). Similarly, optimal pyramiding strategies best combined the proportions of *S* (P_S) and R_{12} ($P_{R_{12}}$) cultivars, either using the same proportion each year (PyS*), or by varying these proportions from year to year (vPyS*).

parameters of the model are listed in Table 2. We will first introduce the model, parameters and hypothesis describing within-host virus dynamics and then the epidemic dynamics in a heterogeneous landscape. We will simplify the presentation of the model here, by focusing on the case $n_c = 2$, in which four cultivars are considered: an S cultivar, two monogenic cultivars R_1 and R_2, and the cultivar pyramiding the two resistances R_{12}. The generalization to $n_c \geq 2$ is given in Supporting Information Notes S1.

Model of within-host virus dynamics

For within-host dynamics, we assume that the pathogen pathotypes coexist in an equilibrium between mutation and selection. With four cultivars, the coexistence frequencies of the four possibles pathotypes (av, v_1, v_2, v_{12}) in each host cultivar depend on m_1 (resp. m_2), the number of point mutations that the wild-type virus variant must accumulate in its genome to break down the qualitative resistance gene R_1 (resp. R_2); s, the fitness cost induced by a single mutation; and κ, the intensity of epistasis between mutation. For $\kappa = 1$, each mutation decreases fitness independently, by the same factor $(1 - s)$ (no epistasis). When $0 < \kappa < 1$, the mean fitness cost of several mutations is lower than that of s (antagonistic mutations), whereas $\kappa > 1$ indicates synergistic mutations (Wilke & Adami, 2001). For viruses, antagonistic epistasis has been reported to be common (Wilke *et al.*, 2003; Sanjuan *et al.*, 2004). The derivation of the coexistence frequencies required the definition of variants of particular interest in the virus population.

As an example, with $m_1 = 1$ and $m_2 = 2$, we have eight variants in the virus population as, at each of the $m_{tot} = m_1 + m_2$ sites, each variant does or does not have the nucleotide required to break down R gene. Each variant sequence can be assigned to one of the four possible pathotypes (av, v_1, v_2, v_{12}) (Table 3a). The fitness of each virus variant in each cultivar is defined with the parameters s and κ (Table 3b). The coexistence frequencies of the variants and corresponding pathotypes can then be obtained following Sasaki & Nowak (2003) and Wilke (2005). Formally, we obtained the mutation-selection balance matrix $\gamma = \left(\gamma_{i,j}\right)_{1 \leq i,j \leq (n_c+2)}$. This matrix is an $(n_c + 2) \times (n_c + 2)$ matrix in which rows correspond to the $(n_c + 2)$ virus pathotypes (av, v_1, v_2, v_{12}) and columns correspond to the $(n_c + 2)$ cultivars S, R_1, R_2, R_{12}. We refer to Notes S2 for more details on the derivation of the matrix γ.

Model of seasonal epidemics in a heterogeneous landscape

Baseline model in a landscape with only the *S* cultivar The model proposed by Fabre *et al.* (2012, 2015) describes the dynamics of $I_{S,y}(t)$, the number of plants infected in a field (sown with the S cultivar) at time t during year y. It takes into account three routes of infection through dedicated parameters: infection of the field from the reservoir (at a rate α_E), infection between

Table 2 Description of the state variables and parameters of the model

State variables		
S	Referring to susceptible cultivar	
R_j	Referring to the j-monogenic resistant cultivar; $j \in \{1, 2, \cdots, n_c\}$	
$R_{12\ldots n_c}$	Referring to cultivar pyramiding n_c monogenic resistances	
$I_{V,y}$	Number of infected plants in a field with V-cultivar during year y, $V \in \{S, R_1, R_2, \cdots, R_{n_c}, R_{12\ldots n_c}\}$	
$\alpha_{V,y}$	Rate of infection of the V-cultivar by reservoir during year y, $V \in \{S, R_1, R_2, \cdots, R_{n_c}, R_{12\ldots n_c}\}$	

Parameters included in the numerical experiment Parameters	Description {reference value}	Unit {value or range}
n_c	Number of cultivars with monogenic resistance {2; 3}	Number {1;2;3;5}
n_y	Number of years of resistance deployment {20}	Year {10;20;40}
λ	Characteristic of the pathogen reservoir {0.5}	Unitless {0.1;0.5;0.9}
Ω_{int}	Epidemic intensity before R deployment	Unitless {0.1 to 0.8} by step of 0.05
Ω_{pfl}	Landscape connectivity before R deployment	Unitless {(0.33, 0.33, 0.33); (0.9, 0.05, 0.05); (0.05, 0.9, 0.05); (0.05, 0.05, 0.9)}
m_j	Number of mutations necessary for breakdown R_j {1}	Number {1;2}[1]
s	Fitness cost of a single mutation {10^{-3}}	Unitless {10^{-3}; 10^{-2}; 10^{-1}}
κ	Epistasis intensity {1}	Unitless {10^{-3}, 0.5, 1, 1.5}

Fixed parameters Parameters	Description {reference value}	Unit
n_d	Duration of the cropping season {120}	Day
n_f	Number of fields in the landscape {400}	Field
n_p	Number of plants in a field 10^4	Plant
μ	Mutation rate {10^{-4}}	Generation^{-1} nucleotide^{-1}

[1]Depending on the number of cultivars with monogenic resistance (n_c), the possible combinations of $m = (m_1, m_2, \ldots, m_{n_c})$ considered for the model simulation are: for $n_c = 1$: $m \in \{1; 2\}$; for $n_c = 2$: $m \in \{(1, 1); (1, 2); (2, 2)\}$; for $n_c = 3$: $m \in \{(1, 1, 1); (1, 1, 2); (1, 2, 2); (2, 2, 2)\}$; for $n_c = 5$: $m \in \{(1, 1, 1, 1, 1); (1, 1, 1, 1, 2); (1, 1, 1, 2, 2); (1, 1, 2, 2, 2); (1, 2, 2, 2, 2); (2, 2, 2, 2, 2)\}$

Table 3 Host–virus interaction matrix and fitness matrix for four plant cultivars (a susceptible cultivar (*S*), two monogenic cultivars (R_1, R_2) and a cultivar pyramiding R_1 and R_2 genes (R_{12})) and the eight virus variants considered when $m_1 = 1$ (resp. $m_2 = 2$) is the number of mutations required for the wild-type virus to break down the resistance conferred by R_1 (resp. R_2) gene

		(a)				(b)			
Variant sequence	Pathotype	*S*	R_1	R_2	R_{12}	*S*	R_1	R_2	R_{12}
000	(*av*)	1	0	0	0	1	0	0	0
100	(v_1)	1	1	0	0	1−*s*	1	0	0
010	(*av*)	1	0	0	0	1−*s*	0	0	0
001	(*av*)	1	0	0	0	1−*s*	0	0	0
110	(v_1)	1	1	0	0	$(1-s)^{2\kappa}$	1-*s*	0	0
011	(v_2)	1	0	1	0	$(1-s)^{2\kappa}$	0	1	0
101	(v_1)	1	1	0	0	$(1-s)^{2\kappa}$	1-*s*	0	0
111	(v_{12})	1	1	1	1	$(1-s)^{3\kappa}$	$(1-s)^{2\kappa}$	1-*s*	1

With $m_1 = 1$ and $m_2 = 2$, three nucleotide sites are considered in the viral genome. A mutation at the first site confers the capacity to infect the R_1 cultivar. Two mutations at the second and third sites are required for infection of the R_2 cultivar. The pathotype of each virus variant is indicated in brackets after the binary sequence. (a) The interaction matrix indicates, for each cultivar, whether infection occurs (1) or not (0) for the $8 = 2^{m_1+m_2}$ variants. (b) The fitness matrix is used to derive the relative frequencies of each virus variant in each host cultivar. In addition to m_1 and m_2, the fitness matrix depends on the fitness cost of a single mutation (*s*) and the epistatic interactions between mutations (κ)

fields (at a rate β_c); and infection within a field (at a rate β_F). Using n_f to denote the number of fields in the landscape, n_p to denote the number of plants in a field and n_d to denote the duration of the cropping season, the model reads:

$$\begin{cases} \dot{I}_{S,y}(t) = (n_p - I_{S,y}(t))\Big(\overbrace{\alpha_E}^{\text{reservoir}} + \overbrace{\beta_F I_{S,y}(t)}^{\text{within field}} + \overbrace{\beta_C (n_f - 1) I_{S,y}(t)}^{\text{between fields}}\Big); \\ \qquad \text{for all } t \in]0, n_d]; y \in \{1, \cdots, n_y\}, \\ I_{S,y}(0) = 0; \quad \text{for all } y \in \{1, \cdots, n_y\}. \end{cases}$$

Eqn 1

In a landscape containing only the *S* cultivar, the reservoir load is constant between seasons and epidemics repeat themselves identically every year. Integrating system Eqn 1, we define the area under the disease progress curve (AUDPC) at the landscape scale as $A_0 = n_f \int_0^{n_d} I_{S,y}(t)\mathrm{d}t$.

Epidemics in an agricultural landscape are intuitively characterized by: the mean epidemic intensity in a field during a season, defined as $\Omega_{\text{int}} = \frac{A_0}{n_f n_p n_d}$; and the relative importance of the three routes of infection $\Omega_{pfl} = \left(\Omega^1_{pfl}, \Omega^2_{pfl}, 1 - \Omega^1_{pfl} - \Omega^2_{pfl}\right)$ (Fabre *et al.*, 2012). The vector Ω_{pfl} captures the infection profile of the landscape, which is dependent on the connectivity between its elements (fields, reservoir). Ω^1_{pfl} is the proportion of infections originating from the reservoir, Ω^2_{pfl} is the proportion of between-field infections and the remaining, $\Omega^3_{pfl} = 1 - \Omega^1_{pfl} - \Omega^2_{pfl}$ is the proportion of within-field infections. Mathematically, we have:

$$\Omega^1_{pfl} = \frac{\alpha_E}{A_0} \int_0^{n_d} \int_0^t (n_p - I_{S,y}(\tau))\mathrm{d}\tau\mathrm{d}t,$$
$$\Omega^2_{pfl} = \frac{\beta_C (n_f - 1)}{A_0} \int_0^{n_d} \int_0^t (n_p - I_{S,y}(\tau)) I_{S,y}(\tau)\mathrm{d}\tau\mathrm{d}t.$$

Eqn 2

Within-season model in a heterogeneous landscape Now, in addition to the susceptible cultivar *S*, let us introduce the three resistant cultivars R_1, R_2 and R_{12}. During year *y*, $P_{V,y}$ is the proportion of fields with cultivar $V \in \{S, R_1, R_2, R_{12}\}$ and $\alpha_{V,y}$ its rate of infection from the reservoir. The model now reads:

$$\begin{bmatrix} \dot{I}_{S,y} \\ \dot{I}_{R_1,y} \\ \dot{I}_{R_2,y} \\ \dot{I}_{R_{12},y} \end{bmatrix} = \mathrm{diag} \begin{bmatrix} n_p - I_{S,y} \\ n_p - I_{R_1,y} \\ n_p - I_{R_2,y} \\ n_p - I_{R_{12},y} \end{bmatrix} \left\{ \overbrace{\begin{bmatrix} \alpha_{S,y} \\ \alpha_{R_1,y} \\ \alpha_{R_2,y} \\ \alpha_{R_{12},y} \end{bmatrix}}^{\text{reservoir}} + \beta_F \overbrace{\begin{bmatrix} I_{S,y} \\ I_{R_1,y} \\ I_{R_2,y} \\ I_{R_{12},y} \end{bmatrix}}^{\text{within field}} + \beta_C \underbrace{\begin{bmatrix} P_{S,y} n_f - 1 & P_{R_1,y} n_f & P_{R_2,y} n_f & P_{R_{12},y} n_f \\ P_{S,y} n_f (\gamma_{21} + \gamma_{41}) & P_{R_1,y} n_f - 1 & P_{R_2,y} n_f \gamma_{43} & P_{R_{12},y} n_f \\ P_{S,y} n_f (\gamma_{31} + \gamma_{41}) & P_{R_1,y} n_f \gamma_{42} & P_{R_2,y} n_f - 1 & P_{R_{12},y} n_f \\ P_{S,y} n_f \gamma_{41} & P_{R_1,y} n_f \gamma_{42} & P_{R_2,y} n_f \gamma_{43} & P_{R_{12},y} n_f - 1 \end{bmatrix}}_{\text{between fields}} \begin{bmatrix} I_{S,y} \\ I_{R_1,y} \\ I_{R_2,y} \\ I_{R_{12},y} \end{bmatrix} \right\},$$

Eqn 3

where *diag*(*x*) is a diagonal matrix in which the diagonal entries are given by *x*, and $\gamma = \left(\gamma_{i,j}\right)_{1 \le i,j \le 4}$ is the mutation-selection balance matrix defined in the previous section.

$I_{V,y}(t)$ is the number of infected plants in a field containing cultivar *V* at time *t* and during year *y*. As each field has a total of n_p plants, $n_p - I_{V,y}$ is the number of healthy plants. Each year, at the beginning of the epidemic, farmers sow healthy plants, that is, $I_{V,y}(0) = 0$ for all *y*, *V*. Again, three routes of infection are considered. First, infections of cultivar *V* are initiated from the reservoir at a rate $\alpha_{V,y}$. Second, by the mass action principle, infections

occur from sources in the same field (and thus of the same cultivar) at rate β_F. Lastly, infections occur from infected plants in any other field at rate β_c. More precisely, this term counts all the infection sources in all remote fields and weights the force of these sources by the coexistence frequencies of the pathotypes able to infect cultivar V.

The genetic structure of the pathogen population can be derived by calculating the proportion of the pathotype frequencies at time t during year y as $\frac{1}{I_y(t)}\gamma \cdot \left(I_{S,y}(t), I_{R_1,y}(t), I_{R_2,y}(t), I_{R_{12},y}(t)\right)^T$, wherein $I_y(t) = I_{S,y}(t) + I_{R_1,y}(t) + I_{R_2,y}(t) + I_{R_{12},y}(t)$.

Between-season model Epidemics in successive cropping seasons are coupled to each other through the interaction of the crop with a reservoir compartment selectively neutral for the pathogen population. Assuming that the migration of propagules of each pathotype from the crop into the reservoir is proportional to the intensities of the overall epidemic in each cultivar during year y, $A_{V,y} = n_f P_{V,y} \int_0^{n_d} I_{V,y}(t)\mathrm{d}t$ (relative to the overall epidemic intensity of a landscape with only S cultivar, A_0), a single additional parameter $\lambda \in]0, 1[$ was required to control the renewal of virus load. High values of λ characterize a reservoir in which the prevalence of the virus pathotypes changes rapidly as a result of short host life spans and small reservoir size. Low values of λ characterize a roughly stable reservoir in which virus dynamics displays marginal dependence on epidemic dynamics in the crops. Therefore, for all $y \in \{2, \ldots, n_y\}$ the interseason dynamics of the viral load of the reservoir is defined by:

$$\begin{bmatrix} \alpha_{S,y} \\ \alpha_{R_1,y} \\ \alpha_{R_2,y} \\ \alpha_{R_{12},y} \end{bmatrix} = (1-\lambda) \begin{bmatrix} \alpha_{S,y-1} \\ \alpha_{R_1,y-1} \\ \alpha_{R_2,y-1} \\ \alpha_{R_{12},y-1} \end{bmatrix} + \lambda \frac{\alpha_E}{A_0} \begin{bmatrix} 1 & 1 & 1 & 1 \\ \gamma_{21}+\gamma_{41} & 1 & \gamma_{43} & 1 \\ \gamma_{31}+\gamma_{41} & \gamma_{42} & 1 & 1 \\ \gamma_{41} & \gamma_{42} & \gamma_{43} & 1 \end{bmatrix} \begin{bmatrix} A_{S,y-1} \\ A_{R_1,y-1} \\ A_{R_2,y-1} \\ A_{R_{12},y-1} \end{bmatrix}. \quad \text{Eqn 4}$$

Initially, before the deployment of resistant cultivars (i.e. at year $y = 1$), the prevalence of the pathotypes in the reservoir depends on their coexistence frequencies in fields planted with the S cultivar. Thus, $(\alpha_{S,1}, \alpha_{R_1,1}, \alpha_{R_2,1}, \alpha_{R_{12},1}) = \alpha_E(1, \gamma_{21}+\gamma_{41}, \gamma_{31}+\gamma_{41}, \gamma_{41})$.

Model analysis

Performance of deployment strategies We aimed to compare the performance of a set of deployment strategies defined in Table 1. The AUDPC, previously defined as $A_{V,y}$, is used as a proxy of yield losses caused by viruses. The performance of a given strategy is then estimated by assessing the damage caused by the pathogen during n_y years in the entire landscape relative to the damage obtained when only the S cultivar is grown (Fabre *et al.*, 2015). For example, a relative damage of 80% means that strategy P decreases the epidemic damage by: 100–80% = 20%.

Formally, a deployment strategy $P = \left(P_{V,1}, \ldots, P_{V,n_y}\right)_{V \in \{S,R_1,R_2,R_{12}\}}$ is the time series of the proportion of fields sown with the different cultivars each year in the landscape. Its performance is

$$\Delta(P, \delta) = \frac{100}{n_y A_0} \times \sum_{y=1}^{n_y} \sum_{V \in \{S,R_1,R_2,R_{12}\}} A_{V,y}(P_{V,y}, \delta); \quad \text{Eqn 5}$$

with the natural condition $\sum_{V \in \{S,R_1,R_2,R_{12}\}} P_{V,y} = 1$ for all $y \in \{1, \ldots, n_y\}$; where $\delta = \left(m, s, \kappa, \Omega_{int}, \Omega_{pfl}, \lambda, n_y\right)$ is a given set of the parameters of interest. Below, the strategy P is considered as an element of the strategies set {MoS, PyS, MoS*, vMoS*, PyS*, vPyS*} (Table 1).

In addition, we defined the difference in performance between two strategies P_1 and P_2 as $D(P_1, P_2) = \Delta(P_1, \delta) - \Delta(P_2, \delta)$ (corresponding to the percentage difference in damage between the two strategies). For example, a positive value of 10% indicates that strategy P_1 is 10% more beneficial than strategy P_2. Negative values indicate that P_2 outperforms P_1.

Numerical experiment The model was implemented in MATLAB and analyzed using the R software (www.r-project.org). Ordinary differential equations were solved using the ODE45 MATLAB solver. The model was explored in a large number of vector parameters δ representative of a wide range of production situations (i.e. the set of physical, biological and socioeconomic factors determining agricultural production). Optimal strategies were identified with the MATLAB nonlinear programming solver FMINCON for each δ considered thereafter. Sensitivity analyses (Saltelli *et al.*, 2008) were performed to estimate the relative importance of the model parameters of interest $\delta = \left(m, s, \kappa, \Omega_{int}, \Omega_{pfl}, \lambda, n_y\right)$ for the yield performance $\Delta(P, \delta)$ of optimal strategies, by running the model over a full factorial design with 19 440 parameter combinations ($n_c = 2$, deployment of two R genes) and 25 920 combinations ($n_c = 3$, deployment of three R genes) (Table 2). Sensitivity indices were calculated as described by Fabre *et al.* (2015). Regression trees were built with the function RPART (R package 'PARTY') to analyze the difference in performance D (Py,MoS) and D (MoS, MoS*). A regression tree was fitted to analyze the difference in performance D (PyS, MoS) obtained with two and three R genes over 45 360 parameter combinations (19 440 for $n_c = 2$ plus 25 920 for $n_c = 3$). In this analysis, D (PyS*, MoS*) was used as an illustrative variable.

Sensitivity analysis and regression trees were also used to assess the effect of increasing the number of R cultivars in mosaic strategies. Eight parameter were considered: n_c, $m|n_c$ (m and n_c are nested factors), s, κ, Ω_{int}, Ω_{pfl}, λ and n_y. A classification tree for D (MoS, MoS*) over a factorial design with 97 200 parameter combinations (i.e. 12 960 ($n_c = 1$) + 19 440 ($n_c = 2$) + 25 920 ($n_c = 3$) + 38 880 ($n_c = 5$)) was fitted. Sensitivity analyses were also performed to estimate the relative importance of these eight parameters for the yield performance of simple and optimal mosaic strategies on a subset of 25 920 parameter combinations. Finally, a regression tree for D (MoS*, vMoS*) was fitted on a

subset of previous parameters combinations, as the optimization procedure was highly time-consuming for variable strategies. In total, we considered 8640 parameter combinations by setting $n_y = 20$ and $m_{tot} = n_c$ (meaning that a single mutation is needed to break down the resistance conferred by a particular R gene).

Results

Typical epidemic dynamics simulated with the model

In the model, the pathogen pathotypes coexist in equilibrium between mutation and selection within their host plants. This is illustrated for the four pathotypes in our follow-up example where, the wild-type virus variant must accumulate $m_1 = 1$ (resp. $m_2 = 2$) mutations in its genome to break down the resistance gene R_1 (resp. R_2) (Fig. 1, Tables S1 and S2 for other mutational pathways). In agreement with the multilocus GFG system (Table 3a), coexistence frequencies are firstly determined by plant genotypes (Fig. 1a). The fitness costs of mutations have a large effect. In an S cultivar, 10% of the variants belong to the resistance-breaking pathotypes v_1, v_2, v_{12} for $s = 10^{-3}$, < 2% belong to these pathotypes for $s = 0.01$ and only 1‰ of them for $s = 0.1$ (Fig. 1b). Coexistence frequencies also depend on the epistasis parameter κ for pathotypes bearing at least two mutations in their genome. Its effect is strongest for the lowest mutation fitness costs ($< 10^{-2}$) (Fig. 1c).

The model describes epidemics during successive cropping seasons in an agricultural landscape with connectivity Ω_{pfl}. In the baseline situation, all the fields are sown with the S cultivar and epidemics repeat themselves identically in each field and every year with mean incidence Ω_{int} (Fig. 2a). Now, let us introduce two resistant cultivars (characterized by $m_1 = 1$, $m_2 = 2$ and $s = 0.1$) and deploy the corresponding optimal mosaic strategy (MoS*) by sowing 16% of the fields with the S cultivar, 31% with cultivar R_1 and 53% with cultivar R_2. Initially, the av pathotype is nearly fixed in the pathogen population but other pathotypes are generated by recurrent mutation according to their coexistence frequencies in the S cultivar (Fig. 2c). In a first stage, the overall epidemic dynamics is decreasing from one season to the next (Fig. 2a) as a result, of: the low epidemics occurring in the fields sown with R_1 and R_2 (as initially their rates of infection from the reservoir are very low); and the concomitant slowing down of epidemics in the fields sown with the S cultivar (corresponding to the reduction of the rate of infection of the S cultivar from the reservoir) (Fig. 2b). At the same time, this process is counteracted by the selection of pathotypes adapted to R_1 and R_2 (Fig. 2c). This result, in a second stage, in an increasing in the overall epidemic dynamics after 10 seasons (Fig. 2a). The area under epidemic dynamics, a proxy of the yield losses caused by virus, was used to compare the performance of the strategies.

Comparison of the different strategies for the deployment of two and three resistance genes

We compared the performance of four deployment strategies: MoS, PyS, MoS* and PyS* (Table 1). With two resistances genes, the simple mosaic strategy (MoS) consists of sowing 50% of the fields with the cultivar R_1 and 50% with R_2 in each year, whereas the simple pyramiding strategy (PyS) consists in sowing 100% of fields with the cultivar R_{12} in each year. The optimal uniform mosaic strategy (MoS*) was based on the best combination of proportions of fields sown with the cultivars S, R_1 and R_2, whereas the optimal uniform pyramiding strategy (PyS*) best combined the proportions of S and R_{12}.

Sensitivity analyses of strategy performance The sensitivity of the relative damage to the seven main model parameters (Table 2)

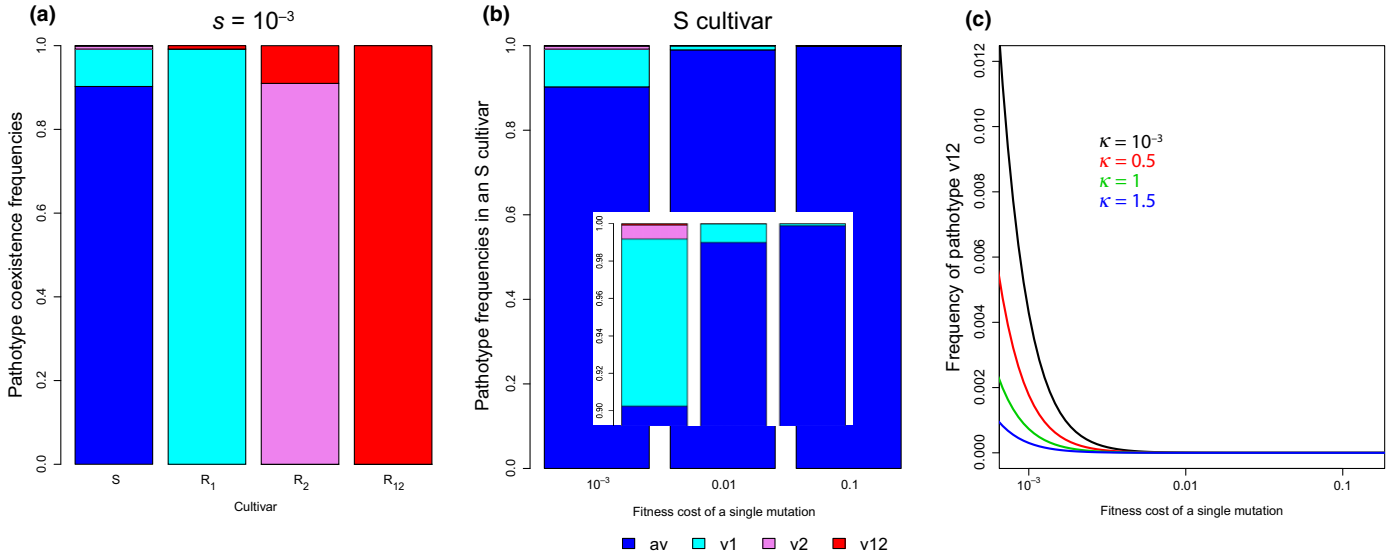

Fig. 1 Coexistence frequencies of the four virus pathotypes considered (av, v_1, v_2, v_{12}) with two resistance genes, R_1 and R_2. A situation where the virus must accumulate one (resp. two) mutation(s) in its genome to break down the resistance conferred by R_1 (resp. R_2) is considered. (a) Effect of the plant cultivar on the coexistence frequencies of the four pathotypes for a fitness cost $s = 10^{-3}$. (b) Effect of the fitness cost of a single mutation s on the coexistence frequencies of the four virus pathotypes in an S cultivar. An embedded zoom graph is provided for frequencies ranging from 0.88 to 1. (c) Effect of the intensity of epistasis κ on the coexistence frequency of the pathotype v_{12} in a S cultivar as a function of the fitness cost of a single mutation s.

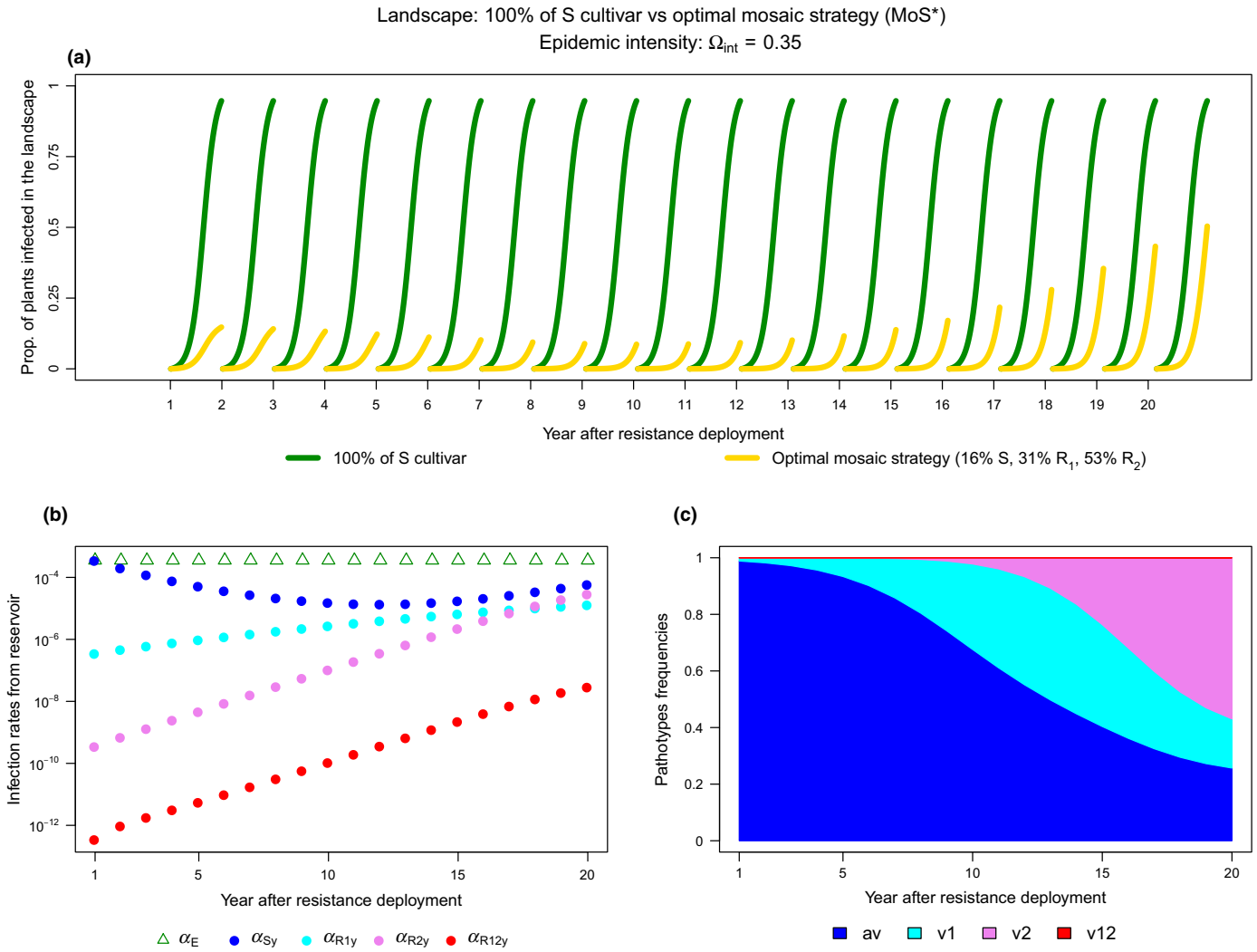

Fig. 2 Typical epidemics simulated by the model. Epidemics are compared between the baseline epidemiological context defined by $\Omega_{pfl} = (0.05, 0.05, 0.9)$ and $\Omega_{int} = 0.35$ in a landscape with only the *S* cultivar and the same landscape where the optimal mosaic strategy (MoS*) obtained with two resistant genes (characterized by $m_1 = 1$, $m_2 = 2$ and $s = 0.1$) is deployed. Other parameters are set to their reference values. The MoS* strategy consists here in sowing 16% of the fields with the *S* cultivar, 31% with cultivar R_1 and 53% with cultivar R_2. (a) Proportion of infected plants (regardless of their cultivars) in the landscape with only the *S* cultivar and with the MoS* strategy deployed during 20 cropping seasons. (b) Interseason dynamics of the rates of infection from the reservoir in the baseline context (α_E) and with the MoS* strategy ($\alpha_{S,y}$, $\alpha_{R1,y}$, $\alpha_{R2,y}$, $\alpha_{R12,y}$). (c) Dynamics of the pathotype frequencies during the cropping seasons with the MoS* strategy.

was assessed independently for the optimal strategies with two and three resistance genes. Three parameters describe the within-host interaction between the virus and the resistance genes considered: the total number of mutations required for the virus to break down the resistance conferred by the n_c genes (m_{tot}), the fitness cost of a single mutation (s) and the intensity of epistasis between mutations (κ). Three other parameters describe the epidemiological dynamics in the landscape before resistance deployment: the mean epidemic intensity in a field during a cropping season (Ω_{int}), the functional connectivity of the landscape (Ω_{pfl}) and the rate of reservoir renewal (λ). The last parameter (n_y) is the number of years during which resistance has been deployed.

The overall picture was very similar for two and three *R* genes, with sensitivity analyses highlighting the importance of the same two main parameters (Ω_{int} and Ω_{pfl}) and secondarily the importance of s for all strategies (Table S3). The sum of the main indices of Ω_{int} and Ω_{pfl} (revealing individual effects) range from 64% (MoS* with three *R* genes) to 72% (PyS* with two *R* genes). The interaction between Ω_{int} and Ω_{pfl} had a marked effect on the PyS* strategy (15% and 18% with two and three genes, respectively), but above all for the MoS* strategies (20% and 30% with two and three *R* genes, respectively). The variance explained by Ω_{int}, Ω_{pfl}, s and their mutual interactions ranges from 90% (PyS* with three *R* genes) to at least 95% (MoS* with two and three *R* genes). By contrast, the four remaining parameters had only a marginal impact on strategy performance, with main effects $\leq 1\%$.

Effect of the three main parameters on strategy performance As the main parameters of the sensitivity analysis are

Ω_{int}, Ω_{pf1} and s, we illustrate the performance of the strategies by plotting the relative damage as a function of $\Omega_{int} \in [0.1, 0.8]$ for two mutation fitness costs (low, $s = 10^{-3}$, and high, $s = 0.1$) in three landscapes differing in terms of the predominant route of infection. We illustrate the case of three R genes (Fig. 3). The corresponding cultivar landscapes underlying the MoS* and PyS* strategies (i.e. proportion of fields sown with each cultivar) and genetic structures of pathogen population (i.e. mean proportion of the pathotypes over the cropping seasons) are illustrated in Fig. S1. Overall, the simple pyramiding strategy (PyS) was

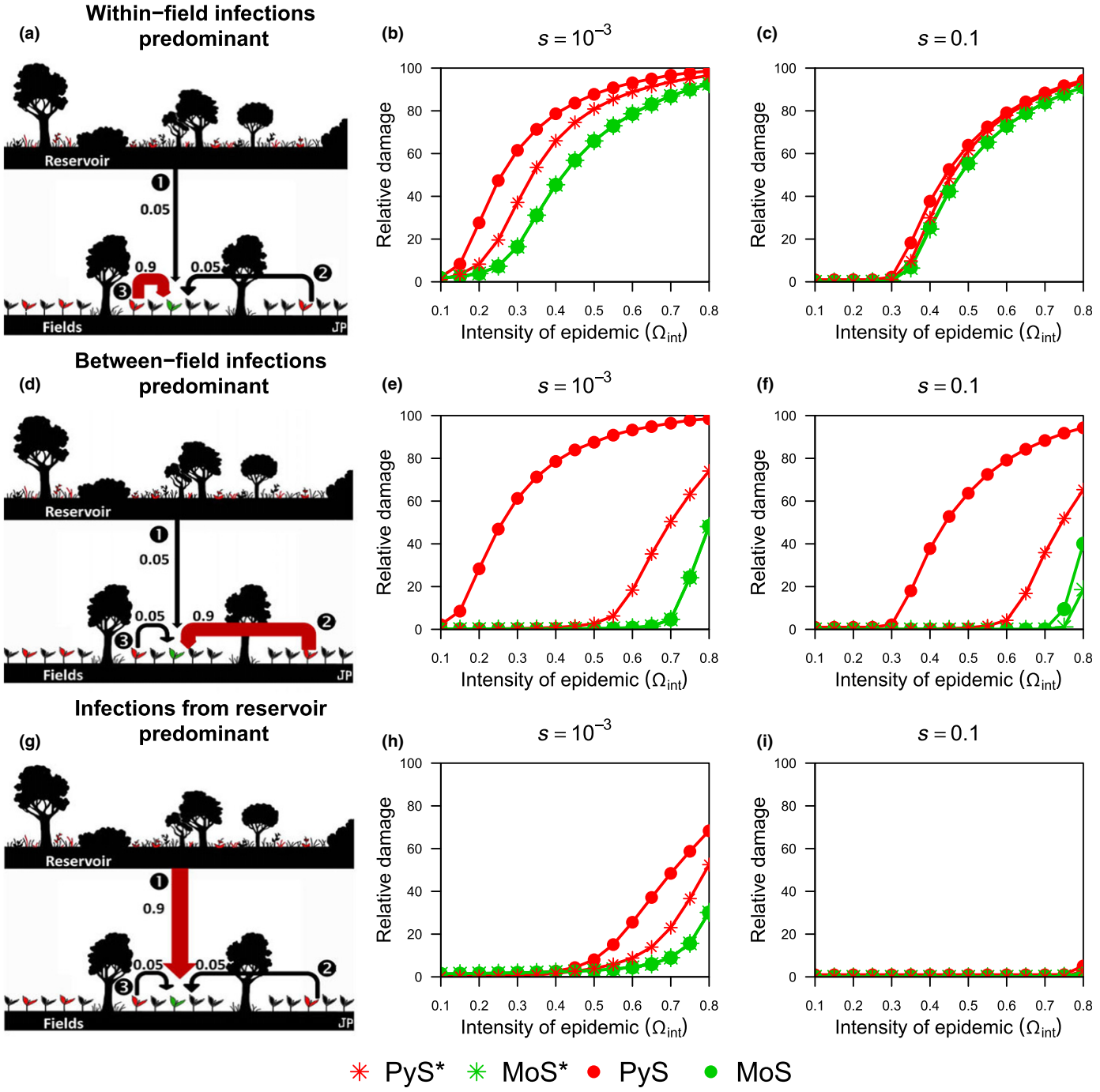

Fig. 3 Damage reduction achieved with mosaic and pyramiding strategies with three resistances genes. The MoS strategy consists of sowing one-third of the fields with each monogenic cultivar R_1, R_2 and R_3, each year. The PyS strategy consists of sowing 100% of fields with cultivar R_{123} each year. The MoS* strategy involved using the proportions of fields sown with the cultivars S, R_1, R_2 and R_3, minimizing pathogen damage. The PyS* strategy involved using the best combination of proportions of S and R_{123}. (a–c) Effect of the fitness costs of mutations s (left $s = 10^{-3}$, right $s = 0.1$) and of epidemic intensity (Ω_{int}) on damage (relative to the damage before resistance deployment) in a landscape in which 90% of infections are within-field infections. (d–f) As for (a–c) but for a landscape in which 90% of infections are between-field infections. (g–i) As for (a–c) but for a landscape in which 90% of infections are initated from the reservoir. Other parameters are set to their reference values. In the landscape drawings (a, d, g) arrows symbolize routes of infection between infected plants (in red) and a focal healthy plant (in green). The dominant route is underlined in red.

often the worst strategy, particularly for the lowest mutation fitness costs. The optimal pyramiding strategy (PyS*) was the next worst strategy. By contrast, the mosaic strategies MoS and MoS* have similar performances, both better than those of the pyramiding strategies.

More precisely, in landscapes dominated by within-field infections (Fig. 3a), none of the strategies gave effective disease control (defined here, arbitrarily, as relative damage ≤ 5%) for the lowest mutation fitness costs and most epidemic intensities ($s = 10^{-3}$ and $\Omega_{int} > 0.2$; Fig. 3b). However, mosaic strategies always performed significantly better than pyramiding strategies. By contrast, for the highest mutation fitness costs ($s = 0.1$; Fig. 3c), all the strategies performed mostly similarly, giving effective disease control for the lowest epidemic intensities ($\Omega_{int} \leq 0.35$).

When between-field infections predominate (Fig. 3d), the difference in performance between PyS, on the one hand, and PyS*, MoS and MoS*, on the other hand, was much greater, whatever the mutation fitness cost. For lower costs, PyS never gave effective disease control, whereas PyS* kept the relative damage to < 5% for $\Omega_{int} \leq 0.55$ and MoS and MoS* kept the relative damage to < 5% for $\Omega_{int} \leq 0.7$ (Fig. 3e). Higher fitness costs (Fig. 3f) differentiated between MoS and MoS* in terms of performance for higher epidemic intensities (> 0.75), with MoS* giving effective disease control for almost all epidemic intensities. Higher fitness costs also improved the performance of PyS, which had a relative damage of < 5% for $\Omega_{int} \leq 0.3$.

In landscapes dominated by infections from the reservoir (Fig. 3g), the disease was fully controlled by all strategies at high fitness cost (Fig. 3i). However, this control was lost in situations of lower fitness cost ($s = 10^{-3}$; Fig. 3h) for $\Omega_{int} \leq 0.5$. For higher intensities, MoS and MoS* performed similarly well, and both were much better than PyS*. Again, the PyS strategy had the worst performance.

The results are nearly similar with strategies combining two *R* genes. However, the MoS and PyS* strategies frequently had quite similar performances. The equivalent of Figs 3 and S1 are provided in Figs S2 and S3.

Mosaic strategies are much more versatile than pyramiding strategies

The differences in performance between mosaic and pyramiding strategies (D (PyS, MoS) and D (PyS*, MoS*) for simple and optimal strategies, respectively) were explored over 45 360 production situations. The analysis covered a wide range of physical × biological × socioeconomic factor combinations typical of agricultural production (Table 2). Overall, mosaic strategies performed at least as well as pyramiding strategies in approximately 92% of the production situations tested. More precisely, MoS* outperformed PyS* (D (PyS*, MoS*)> 2%) in 34% of the production situations and MoS* and PyS* performed approximately similarly ($-2\% \leq D$ (PyS*, MoS*) $\leq 2\%$) in 59% of the production situations. Similarly, simple MoS outperformed PyS in 48% of the production situations tested, whereas these two strategies performed similarly well in 43% of production situations. Finally, pyramiding strategies were more beneficial than mosaic strategies in 7% and 9% of cases for the optimal and simple strategies, respectively.

A regression tree was constructed to identify parameter combinations explaining the difference in performance between strategies (Fig. 4). This tree was built with D (PyS, MoS), with D (PyS*, MoS*) used as an illustrative variable. The parameters identified were the same as those revealed by the sensitivity analysis (Ω_{int}, Ω_{pfl} and s) plus λ and n_y. The tree mainly contrasts landscapes dominated by between-field infections (right branch of the tree) with other patterns of functional connectivity. MoS strategies are much more beneficial than PyS when between-field infections predominate. Optimal MoS* strategies were also better for higher epidemic intensities ($\Omega_{int} \geq 0.32$). For other connectivity patterns, MoS and MoS* tended to be more beneficial than PyS and PyS* for reservoirs displaying moderately rapid or rapid renewal of their viral loads ($\lambda \geq 0.5$), especially for the lowest range of fitness cost ($s \leq 0.01$) when long-term deployment strategies are planned ($n_y = 40$ yr). By contrast, the differences in performance reduce for reservoirs displaying only slow renewal of their viral load ($\lambda = 0.1$) and for shorter-term deployment strategies ($n_y \leq 20$ yr) but remain (on average) in favor of mosaics strategies.

Effect of cultivar diversity on disease control

As mosaic strategies are highly versatile, we explored the effect of the number of *R* cultivars present in the mosaic strategy on disease control. The levels of disease control achieved with optimal or simple mosaic strategies were mostly determined by the same two factors highlighted earlier (Ω_{int}, Ω_{pfl}) plus cultivar diversity (n_c). These three factors alone explained 67% of the relative damage variability obtained (for both MoS and MoS*). These figures rose to 91% (MoS) and 94% (MoS*) if mutual second- and third-order interactions were taken into account. The fourth most important was far behind the fitness cost of a single mutation (s).

When the number of *R* cultivars was increased from one to five, optimal mosaic strategies largely improved disease control, particularly in landscapes dominated by between-field infections or infections from the reservoir, and when mutations breaking down the resistance conferred by *R* genes had low fitness costs (Fig. 5e,h). With higher fitness costs, a high level of disease control was already achieved with mosaics of three *R* cultivars (Fig. 5f,i), and little additional benefit could therefore be gained from increasing the number of *R* genes in the mosaic strategy. Conversely, when within-field infections predominated, disease remained difficult to control even with optimal mosaics of five *R* cultivars. Increasing *R*-gene diversity clearly increased the efficacy of control, but, even with high fitness costs of mutations, an optimal mosaic of five *R* cultivars yielded effective disease control (i.e. relative damage ≤ 5%) only for epidemic intensities ≤ 0.4 (Fig. 5c).

Simple (MoS) and optimal mosaic (MoS*) strategies including three or five *R* cultivars performed similarly (performance difference D (MoS, MoS*) ≤ 2%) in 94% of the production situations tested (Fig. S4). With only two *R* genes, optimal mosaics generally outperformed simple mosaics for the highest range of

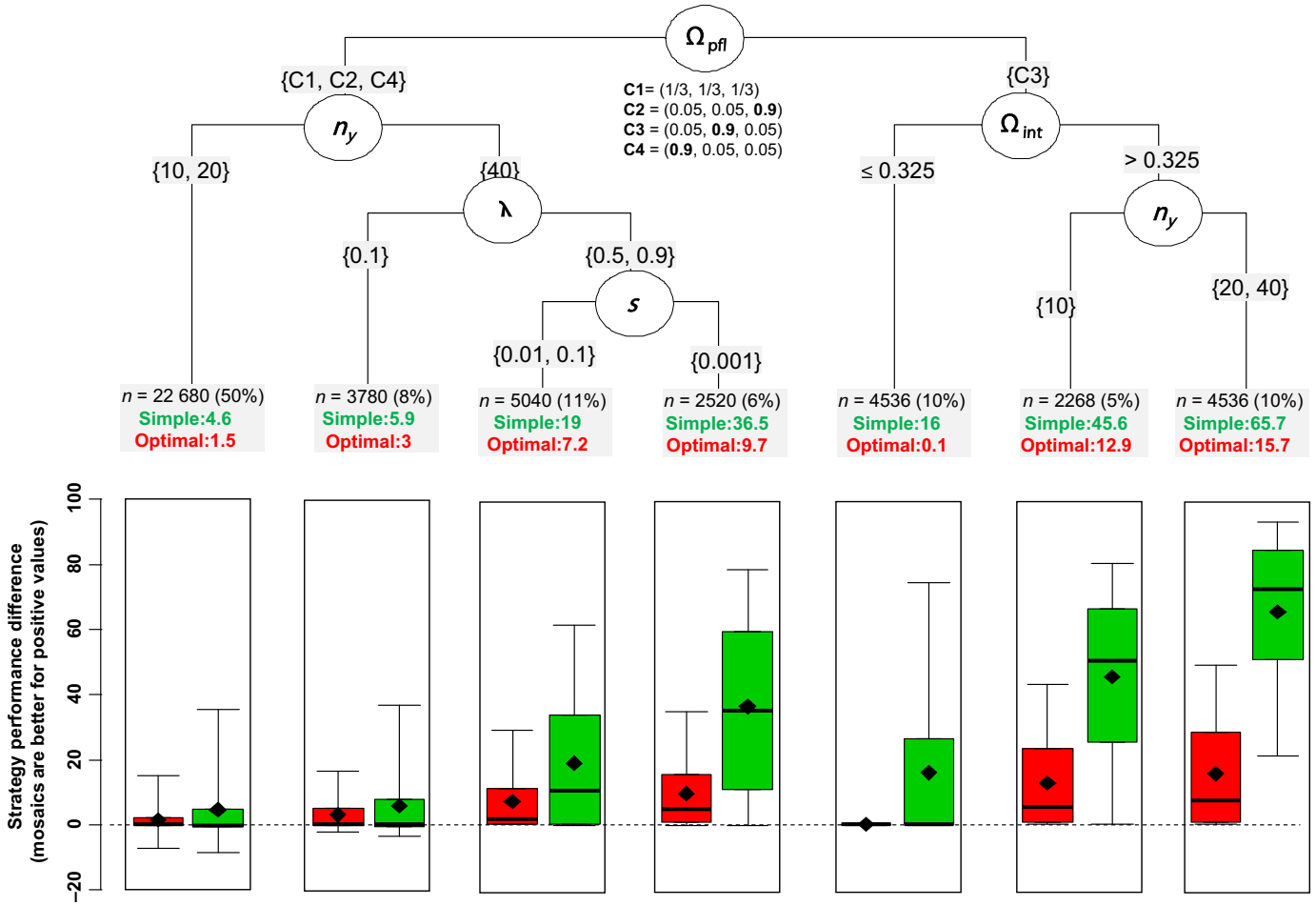

Fig. 4 Regression tree for the difference in performance between mosaic and pyramiding strategies obtained with two and three monogenic resistances, for 45 360 production situations. Production situations correspond to a full-factorial design of the eight main model parameters (Table 2). Positive values indicate that the mosaic performed better than the pyramiding strategies. For each node, the number of production situations is indicated, together with the means for *D* (PyS, MoS) (in green, simple strategies) and *D* (PyS*, MoS*) (in red, optimal strategies). Box plots show the 5%, 25%, 50%, 75% and 95% percentiles of the distribution of *D* (PyS*, MoS*) and *D* (PyS, MoS). The factors identified by the tree are the intensity of the epidemic before deployment (Ω_{int}), landscape connectivity (Ω_{pfl}), the fitness cost of a single mutation (*s*), the reservoir renewal rate (λ) and the number of years of resistance deployment (n_y).

epidemic intensities ($\Omega_{int} \geq 0.6$) and when the relative contribution of between-field infections was ≥33% (Fig. S4). Finally, with a single *R* cultivar, MoS* strategies outperformed simple mosaics in 65% of the production situations tested.

Additional benefit of vMoS* over MoS* and MoS

The optimal uniform mosaic strategy (MoS*) was extended to obtain the optimal variable mosaic strategy (vMoS*), in which the proportions of the cultivars can change from year to year (Table 1). *D* (MoS*, vMoS*), the percentage additional yield of the vMoS* strategy over MoS*, was ≤2% in 76% of the 8640 production situations simulated. Additional yield was substantial only for production situations in which within-field infections predominated, especially when the reservoirs rapidly renew their viral load $\lambda = 0.9$ (Fig. S5). In this case, the mean value of *D* (MoS*, vMoS*) was approximately 6% when $\Omega_{int} < 0.325$ and increased to 21% (resp. 39%) when $\Omega_{int} \geq 0.325$ with strategies including one or two (resp. three or five) *R* cultivars.

Discussion

We addressed the question of whether a set of *R* genes would last longer when stacked into the same plant cultivar or when deployed individually in landscape mosaics. By sharp contrast with the many studies dealing with the best way to combine pharmaceutical drugs or pesticides (REX Consortium, 2013), this question has been little investigated in studies dealing with the durability of plant resistance (REX Consortium, 2016). In a recent review, Burdon *et al.* (2014) noted that 'what is lacking are careful assessments, using ecological and evolutionary principles, of the most effective disease resistance deployment strategies that will maximize both the short-term and the longer-term evolutionary benefits of different combination strategies'. One of the main reasons for this is that most theoretical studies dealing with resistance durability consider only one susceptible and one resistant cultivar *e.g.* (van den Bosch & Gilligan, 2003; Skelsey *et al.*, 2010; Fabre *et al.*, 2012, 2015; Lo Iacono *et al.*, 2013; Papaïx *et al.*, 2013, 2014a,b), making it impossible to compare strategies

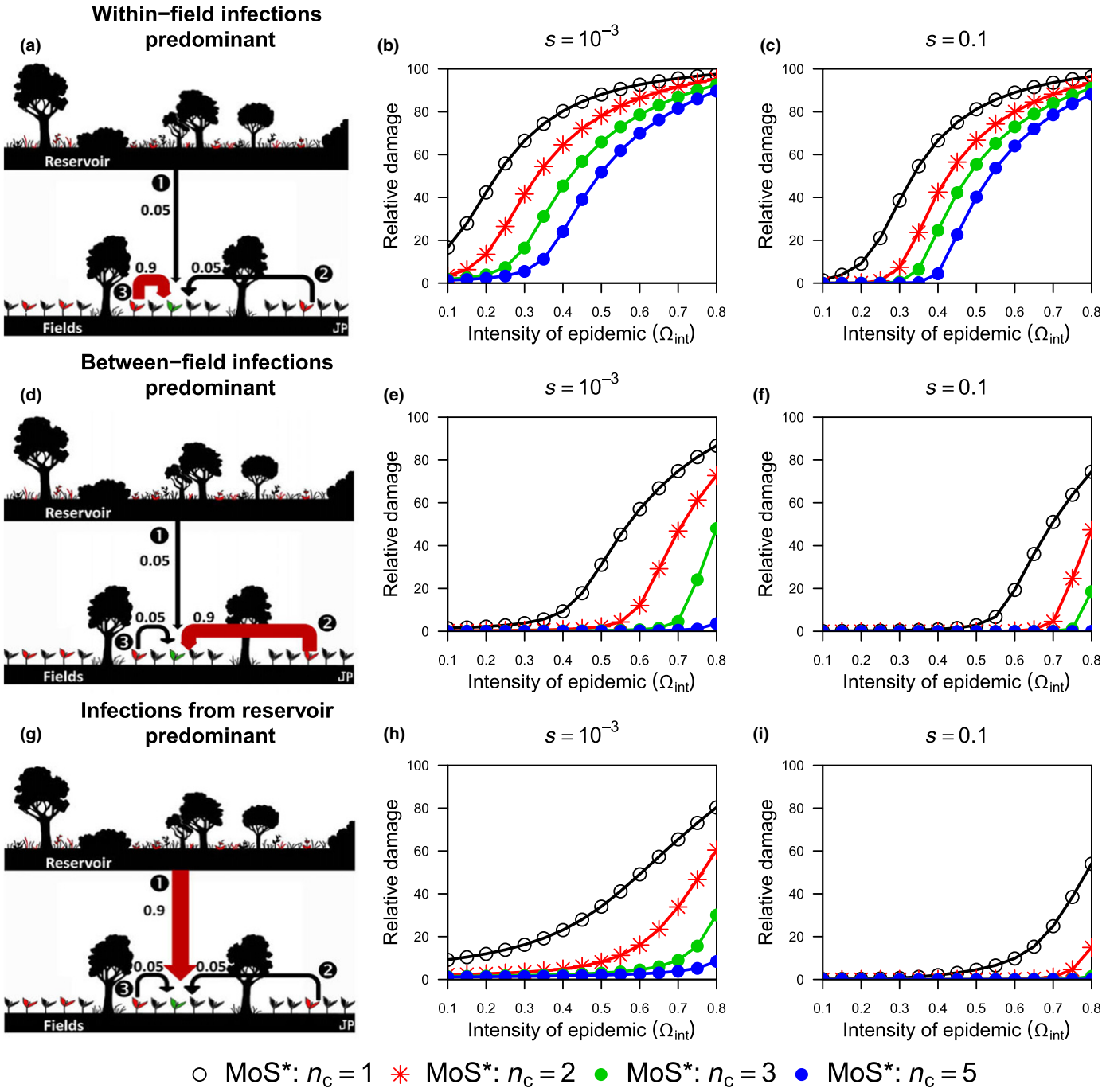

Fig. 5 Damage reduction achieved by deploying an increasing number of one, two, three and five monogenic resistant cultivars in optimal mosaic strategies (MoS*). (a–c) Effect of the fitness costs of mutations s (left $s = 10^{-3}$, right $s = 0.1$) and of epidemic intensity (Ω_{int}) on the epidemic damage (relative to the damage before resistance deployment) in a landscape in which 90% of infections are within-field infections. (d–f) As for (a–c) but for a landscape in which 90% of infections are between-field infections. (g–i) As for (a–c) but for a landscape in which 90% of infections are initiated from the reservoir. Other parameters are set to their reference values. In the landscape drawings (a, d, g) arrows symbolize routes of infection between infected plants (in red) and a focal healthy plant (in green). The dominant route is underlined in red.

deploying more than one resistance gene. We extended the model proposed by Fabre *et al.* (2012, 2015) for a single-locus di-allelic gene-for-gene system to a multilocus system involving an interaction matrix for at least three pathogen variants and as many resistant cultivars. The model links the genetic and epidemiological processes, shaping, at the within- and between-host scales, the demogenetic dynamics of a plant virus in a landscape composed of many fields subject to seasonality and with a reservoir containing viruses year-round.

Mosaic strategies are more versatile

We show here that mosaic strategies are much more versatile than pyramiding strategies. At the landscape scale, mosaic strategies

were at least as good as pyramiding strategies in about 92% of the production situations tested. Our model assumed that the virulence-causing viral mutations at different loci were independent, and the *R* genes had not been deployed before (i.e. no prior pathogen adaptation in the sense that initially the avirulent pathotype is nearly fixed), two conditions favoring the durability of *R* gene pyramids (Mundt, 1990; REX Consortium, 2013, 2016; Brown, 2015). Theoretical studies of coevolution under multilocus gene-for-gene models in natural plant–pathogen systems have already suggested that the use of mixtures of single-resistance gene genotypes is better than the use of multiple resistance alleles in the same cultivar (Sasaki, 2000; Segarra, 2005). These studies, based on population genetics theory, ignored the epidemiological dynamics and considered only natural coevolution, which is disrupted by agriculture. To our knowledge, only Sapoukhina *et al.* (2009) have linked epidemiological and population genetics dynamics to compare mosaic and pyramiding strategies in an agricultural context. They demonstrated that random mixtures of cultivars with monogenic resistance controlled epidemics as efficiently as the pyramiding of *R* genes. Their analysis was restricted to a few epidemiological contexts and could not disentangle the roles of epidemic intensity and landscape connectivity. These findings, and our own results, contrast with the review of REX Consortium (2013) suggesting that combinations of xenobiotics (equivalent to pyramiding in our case study) usually outperform mosaics. In seven theoretical studies comparing combinations and mosaics, they found that the combination outperformed the mosaic in five studies, the mosaic was better than the combination in one study, and the result depended on the model parameters in the remaining study. Insightful comparisons are difficult, as model structures and hypotheses, and the criteria used to compare strategies differ considerably between these studies.

Mosaic strategies outperform pyramiding strategies when: between-field infections predominate, epidemic intensities (before *R* cultivar deployment) are high, and the fitness costs associated with adaptive mutations in the virus are low (Fig. 4). Simple mosaics operate in two principal ways. First, they operate through an epidemiological mechanism analogous to the dilution effect (Plantegenest *et al.*, 2007), a mechanism initially described in cultivar mixtures within fields (Wolfe, 1985; Mundt, 2002). Note that the other two mechanisms put forward by Wolfe (1985) to explain the lower levels of disease in mixtures do not operate in our model: barrier effects resulting from differences in plant architecture between resistant and susceptible cultivars and induced resistance. In our setting, the higher the frequency of between-field infection events and epidemic intensities, the higher the dilution effect. The second principle through which mosaics operate is an evolutionary mechanism, known as disruptive selection (i.e. mosaics create a selection environment favoring different pathogen genotypes at different places; McDonald & Linde, 2002; Zhan *et al.*, 2015). The intensity of disruptive selection is determined by tradeoffs in the adaptation of the different virus variants to the different hosts, a factor classically highlighted by theoretical works on adaptation in heterogeneous environments (e.g. Gandon 2002, Ravigné *et al.* 2009, Débarre & Gandon 2010). As fitness costs increase, so does the disruptive selection imposed on the pathogen population. Fitness costs are not systematic, but they do occur in many plant–pathogen interactions (Zhan *et al.*, 2015), particularly those involving plant viruses (Sacristan & Garcia-Arenal, 2008), in which they are often high (Carrasco *et al.*, 2007; Sanjuan, 2010; Fraile *et al.*, 2011; García-Arenal & Fraile, 2013). The other two parameters determining these tradeoffs, the number of mutations necessary for *R* breakdown (m) and the nature and intensity of epistasis between adaptive mutations (κ) had marginal effects on the performance of strategies at landscape scale. Brown (2015) recently suggested that synergy between the effects of costly mutations ($\kappa > 1$ in our setting; i.e. fitness penalty is an accelerating function of the number of mutations) can theoretically account for the higher durability of *R* gene pyramids. This parameter does not appear to be determining in our model, as its effect remained smaller than that of s and vanished as soon as $s \geq 5 \times 10^{-3}$ (Fig. 1c).

Pyramiding strategies outperformed mosaics in one particular specific context: low values of λ characterizing virus dynamics in the reservoir largely uncoupled from virus dynamics in the crops. This situation occurs, for example, when the host reservoir is much larger than that of the cultivated compartment, or if the reservoir compartment is somewhat separated from the cultivated compartment of the landscape. Unlike simple mosaic strategies, simple pyramiding strategies have only one mode of operation, at the very first step in the emergence of a multi-virulent variant. Pyramids operate by reducing the probability of multivirulent variants emerging and being transmitted. According to the model, the more costly and complex the mutational pathways leading to multivirulence, the less likely they are to be transmitted. Simple pyramids involve no dilution effect and exert no disruptive selection. With an optimal pyramid, the use of the *S* cultivar makes it possible to mobilize these mechanisms to at least some extent. Consistent with these mechanisms, we found that a simple mosaic strategy outperformed the simple pyramid strategy in 48% of the production situations tested and performed similarly well in 43% of production situations. However, the optimal mosaic strategy outperformed the optimal pyramid strategy in only 34% of production situations and performed similarly in 59%.

The level of diversity in the mosaic strategy

The genetic diversity of hosts limits the spread of epidemics in a wide range of conditions, in both natural (Ostfeld & Keesing, 2012) and managed ecosystems (Mundt, 2002; Garrett *et al.*, 2009). The number of *R* components required to obtain efficient disease control has been largely overlooked. To our knowledge, only Mikaberidze *et al.* (2015) have investigated the dependence of the optimal number of cultivars in mixtures on the degree of host specialization and pathogen transmission rate. For markedly specialized pathogens, mimicking GFG interactions with high fitness costs, three-component mixtures effectively achieve a relative damage of $\leq 5\%$ with low to intermediate transmission rates. By contrast, 10–15 components are required for pathogens with

high transmission rates (Mikaberidze *et al.*, 2015). We obtained similar results, despite the differences in our model structure. Three to five *R* genes were sufficient in diverse production situations in which between-field infections or infections from the reservoir predominated (Fig. 5d–i). Our results suggest that much larger numbers of components would be needed at high epidemic intensities in landscapes dominated by within-field infections, as the additional disease control increased very slowly with diversity (Fig. 5a–c). This situation is likely to be common, as pathogen dispersal is often characterized by a highly local dispersal component and rare long-distance dispersal component (Wingen *et al.*, 2013). Thus, for successful control, the increase in cultivar diversity should be accompanied by the planting of crops in smaller fields (i.e. increasing the number of plant genotype units and decreasing their unit area, as pointed out by Mundt, 1988).

Simple (MoS) and optimal (MoS*) mosaic strategies including three or five *R* cultivars performed similarly well (meaning that their performance difference was $\leq 2\%$ in 94% of the productions situations tested; Fig. S4). This is important in practice, as simple strategies are defined *a priori*, regardless of the specific production situation. All control approaches must be practical and economically attractive if they are to be adopted (Zhan *et al.*, 2015). We assumed that all *R* genes were identical in terms of the number of adaptive mutations, fitness cost and epistasis level. However, if fitness costs differ between two *R* genes, then the *R* gene imposing the higher fitness cost should probably be preferred, to optimize disease control. The a priori design of mosaic strategies when the fitness costs of adaptive mutations in the virus vary according to the *R* gene used should be investigated further.

Main model hypothesis and limitations

The model ignores recombination in the virus genome, a mechanism likely to disadvantage pyramid strategies (Burdon *et al.*, 2014; Mundt, 2014; Brown, 2015) as it can combine adaptive mutations present in different virus variants. The importance of this mechanism is unclear. In particular, recombination probably has only a minor effect on the rate of acquisition of adaptive mutations in populations with effective population sizes (N_e) of 1000 or less (Althaus & Bonhoeffer, 2005), as adaptive mutations are typically sequentially fixed. Viruses often have very small effective population sizes because of the bottlenecks occurring at many steps of the virus cycle in the plant (Gutiérrez *et al.*, 2012). In this respect, like most models dealing with the evolution of resistance to xenobiotics (REX Consortium, 2010), the model assumed an infinite pathogen population size. Consequently, even if the avirulent pathotype is nearly fixed, all other virulence alleles are assumed to be present initially according to the mutation-selection balance hypothesis. In real populations, some combinations of virulence alleles may be missing as a result of the low N_e. The current model thus ignores the effect of genetic drift on pathogen evolution within and between plants; and the time required for mutations to occur, a factor favoring pyramids. Finally, mutation fitness costs are assumed to be constant, implying an absence of compensatory mutation in the virus genome and that the resistance-breaking mutants revert to their initial frequencies after removal of the *R* gene. This is consistent with observations (or inferences) for some viruses (Harrison, 2002; Janzac *et al.*, 2010; Fraile *et al.*, 2011), but is not a general rule for plant pathogens (Torres-Barcelo *et al.*, 2010; Mundt, 2014).

At a larger scale, we assumed that the relative frequencies of the nonadapted and resistance-breaking variants arising from crops remained unchanged during their stay in the reservoir compartment, which was therefore considered to be selectively neutral. This is clearly a baseline hypothesis, but little evidence is available to affirm or refute it. Natural populations of wild host plants are highly patchy, with many diverse genotypes of the same species, and different environmental conditions between populations (Zhan *et al.*, 2015). Wild hosts are also the main source of disease resistance in crops, and they contain a large diversity of *R* genes and alleles. All these factors make strong directional selection of one particular pathogen variant over another unlikely. More generally, this point highlights the need for further theoretical research at the agro-ecological interface (Papaïx *et al.*, 2015). Even more importantly, experiments at this scale to compare deployment strategies in long-term experiments, as advised by Burdon *et al.* (2014), are required to test current theoretical models, although such experiments are notoriously difficult. Finally, our findings suggest that benefits should be expected from both high-technology solutions facilitating *R*-gene stacking and low-technology solutions promoting diversity or landscaping in agrosystems. The combination of these approaches may provide added value.

Acknowledgements

R.D.D. received support from the Conseil Interprofessionnel du Vin de Bordeaux (CIVB) under the CIVB project 'Recherche, expérimentation, études et outils', and from the EU in the framework of the Marie-Curie FP7 COFUND People Programme, through the award of an AgreenSkills/AgreenSkills+ fellowship under grant agreement number FP7-609398. We thank the anonymous referees for their comments and valuable suggestions.

Author contributions

R.D.D., B.M. and F.F. planned and designed the research. R.D-D. and F.F. wrote the model, and conducted and analyzed the numerical experiments. R.D-D., B.M. and F.F. wrote the manuscript.

References

Althaus CL, Bonhoeffer S. 2005. Stochastic interplay between mutation and recombination during the acquisition of drug resistance mutations in human immunodeficiency virus type 1. *Journal of Virology* **79**: 13572–13578.

van den Bosch F, Gilligan CA. 2003. Measures of durability of resistance. *Phytopathology* **93**: 616–625.

Brown JKM. 2015. Durable resistance of crops to disease: a Darwinian perspective. *Annual Review of Phytopathology* **53**: 513–539.

Burdon JJ, Barrett LG, Rebetzke G, Thrall PH. 2014. Guiding deployment of resistance in cereals using evolutionary principles. *Evolutionary Applications* **7**: 609–624.

Carrasco P, de la Iglesia F, Elena SF. 2007. Distribution of fitness and virulence effects caused by single-nucleotide substitutions in Tobacco etch virus. *Journal of Virology* **81**: 12979–12984.

Débarre F, Gandon S. 2010. Evolution of specialization in a spatially continuous environment. *Journal of Evolutionary Biology* **23**: 1090–1099.

Fabre F, Rousseau E, Mailleret L, Moury B. 2012. Durable strategies to deploy plant resistance in agricultural landscapes. *New Phytologist* **193**: 1064–1075.

Fabre F, Rousseau E, Mailleret L, Moury B. 2015. Epidemiological and evolutionary management of plant resistance: optimizing the deployment of cultivar mixtures in time and space in agricultural landscapes. *Evolutionary Applications* **8**: 919–932.

Flor HH. 1971. Current status of the gene-for-gene concept. *Annual Review of Phytopathology* **9**: 275–296.

Fraile A, Pagán I, Anastasio G, Sáez E, García-Arenal F. 2011. Rapid genetic diversification and high fitness penalties associated with pathogenicity evolution in a plant virus. *Molecular Biology and Evolution* **28**: 1425–1437.

Gandon S. 2002. Local adaptation and the geometry of host-parasite covolution. *Ecology Letters* **5**: 246–256.

García-Arenal F, Fraile A. 2013. Trade-offs in host range evolution of plant viruses. *Plant Pathology* **62**: 2–9.

García-Arenal F, McDonald BA. 2003. An analysis of the durability of resistance to plant viruses. *Phytopathology* **93**: 941–952.

Garrett KA, Zúñiga LN, Roncal E, Forbes GA, Mundt CC, Su Z, Nelson RJ. 2009. Intraspecific functional diversity in hosts and its effect on disease risk across a climatic gradient. *Ecological Applications* **19**: 1868–1883.

Gutiérrez S, Michalakis Y, Blanc S. 2012. Virus population bottle necks during within-host progression and host-to-host transmission. *Current Opinion in Virology* **2**: 546–555.

Harrison BD. 2002. Virus variation in relation to resistance-breaking in plants. *Euphytica* **124**: 181–192.

Janzac B, Montarry J, Palloix A, Navaud O, Moury B. 2010. A point mutation in the polymerase of *Potato virus Y* confers virulence toward the *Pvr4* resistance of pepper and a high competitiveness cost in susceptible cultivar. *Molecular Plant–Microbe Interactions* **23**: 823–830.

Lo Iacono G, van den Bosch F, Gilligan CA. 2013. Durable resistance to crop pathogens: an epidemiological framework to predict risk under uncertainty. *PLoS Computational Biology* **9**: e1002870.

McDonald BA, Linde C. 2002. Pathogen population genetics, evolutionary potential, and durable resistance. *Annual Review of Phytopathology* **40**: 349–379.

Mikaberidze A, McDonald BA, Bonhoeffer S. 2015. Developing smarter host mixtures to control plant disease. *Plant Pathology* **64**: 996–1004.

Mundt CC. 1988. Influence of number of host genotype units on the effectiveness of host mixtures for disease control: a modeling approach. *Phytopathology* **78**: 1087.

Mundt CC. 1990. Probability of mutation to multiple virulence and durability of resistance gene pyramids. *Phytopathology* **80**: 221–223.

Mundt CC. 1991. Probability of mutation of multiple virulence and durability of resistance gene pyramids: further comments. *Phytopathology* **81**: 240–242.

Mundt CC. 2002. Use of multiline cultivars and cultivar mixtures for disease management. *Annual Review of Phytopathology* **40**: 381–410.

Mundt CC. 2014. Durable resistance: a key to sustainable management of pathogens and pests. *Infection, Genetics and Evolution* **14**: 1348–1567.

Ostfeld RS, Keesing F. 2012. Effects of host diversity on infectious disease. *Annual Review of Ecology, Evolution, and Systematics* **43**: 157–182.

Palumbi SR. 2001. Humans as the world's greatest evolutionary force. *Science* **293**: 1786–1790.

Papaïx J, Adamczyk-Chauvat K, Bouvier A, Kiêu K, Touzeau S, Lannou C, Monod H. 2014a. Pathogen population dynamics in agricultural landscapes: the Ddal modelling framework. *Infection, Genetics and Evolution* **27**: 509–520.

Papaïx J, Burdon JJ, Lannou C, Thrall PH. 2014b. Evolution of pathogen specialisation in a host metapopulation: joint effects of host and pathogen dispersal. *PLoS Computational Biology* **10**: e1003633.

Papaïx J, Burdon JJ, Zhan J, Thrall PH. 2015. Crop pathogen emergence and evolution in agro-ecological landscapes. *Evolutionary Applications* **8**: 385–402.

Papaïx J, David O, Lannou C, Monod H. 2013. Dynamics of adaptation in spatially heterogeneous metapopulations. *PLoS ONE* **8**: e54697.

Plantegenest M, Le May C, Fabre F. 2007. Landscape epidemiology of plant diseases. *Journal of the Royal Society Interface* **16**: 963–972.

Ravigné V, Dieckmann U, Olivieri I. 2009. Live where you thrive: joint evolution of habitat choice and local adaptation facilitates specialization and promotes diversity. *American Naturalist* **174**: E141–E169.

REX Consortium. 2010. The skill and style to model the evolution of resistance to pesticides and drugs. *Evolutionary Applications* **3**: 375–390.

REX Consortium. 2013. Heterogeneity of selection and the evolution of resistance. *Trends in Ecology & Evolution* **28**: 110–118.

REX Consortium. 2016. Combining selective pressures to enhance the durability of disease resistance genes. *Frontiers in Plant Science* **7**: 1916.

Sacristan S, Garcia-Arenal E. 2008. The evolution of virulence and pathogenicity in plant pathogen populations. *Molecular Plant Pathology* **9**: 369–384.

Saltelli A, Ratto M, Andres T, Campolongo F, Cariboni J, Gatelli D, Saisana M, Tarantola S. 2008. *Global sensitivity analysis.* Chichester, UK: Wiley.

Sanjuan R. 2010. Mutational fitness effects in RNA and single-stranded DNA viruses: common patterns revealed by site-directed mutagenesis studies. *Philosophical Transactions of the Royal Society of London B: Biological Sciences* **365**: 1975–1982.

Sanjuan R, Moya A, Elena SF. 2004. The contribution of epistasis to the architecture of fitness in an RNA virus. *Proceedings of the National Academy of Sciences, USA* **101**: 15376–15379.

Sapoukhina N, Durel CE, Le Cam B. 2009. Spatial deployment of gene for-gene resistance governs evolution and spread of pathogen populations. *Theoretical Ecology* **2**: 229–238.

Sasaki A. 2000. Host-parasite coevolution in a multilocus gene-for-gene system. *Proceedings of the Royal Society of London. Series B: Biological Sciences* **267**: 2183–2188.

Sasaki A, Nowak MA. 2003. Mutation landscapes. *Journal of Theoretical Biology* **224**: 241–247.

Segarra J. 2005. Stable polymorphisms in a two-locus gene-for-gene system. *Phytopathology* **95**: 728–736.

Skelsey P, Rossing WAH, Kessel GJT, van der Werf W. 2010. Invasion of *Phytophthora infestans* at the landscape level: how do spatial scale and weather modulate the consequences of spatial heterogeneity in host resistance? *Phytopathology* **100**: 1146–1161.

Torres-Barcelo C, Daros JA, Elena SF. 2010. Compensatory molecular evolution of HC-Pro, an RNA-silencing suppressor from a plant RNA virus. *Molecular Biology and Evolution* **27**: 543–551.

Wilke C. 2005. Quasispecies theory in the context of population genetics. *BMC Evolutionary Biology* **5**: 44.

Wilke CO, Adami C. 2001. Interaction between directional epistasis and average mutational effects. *Proceedings of the Royal Society of London B: Biological Sciences* **268**: 1469–1474.

Wilke CO, Lenski RE, Adami C. 2003. Compensatory mutations cause excess of antagonistic epistasis in RNA secondary structure folding. *BMC Evolutionary Biology* **3**: 3.

Wingen LU, Shaw MW, Brown JKM. 2013. Long-distance dispersal and its influence on adaptation to host resistance in a heterogeneous land scape. *Plant Pathology* **62**: 9–20.

Wolfe MS. 1985. The current status and prospects of multiline cultivars and variety mixtures for disease resistance. *Annual Review of Phytopathology* **23**: 251–273.

Zhan J, Thrall PH, Papaïx J, Xie L, Burdon JJ. 2015. Playing on a pathogen's weakness: using evolution to guide sustainable plant disease control strategies. *Annual Review of Phytopathology* **53**: 19–43.

Supporting Information

Additional Supporting Information may be found online in the Supporting Information tab for this article:

Fig. S1 Cultivar landscape and pathotypes frequencies associated to Fig. 3.

Fig. S2 Damage reduction achieved with mosaic and pyramiding strategies with two resistances genes.

Fig. S3 Cultivar landscape and pathotypes frequencies associated to Fig. S2.

Fig. S4 Classification tree modelling the performance difference between simple and optimal mosaic strategies (MoS vs MoS*) for an increasing number of R cultivars (1, 2, 3 and 5).

Fig. S5 Regression tree modelling the performance difference between the uniform mosaic (MoS*) and the optimal variable mosaic (vMoS*) strategies.

Table S1 Pathotypes coexistence frequencies with two resistance genes

Table S2 Pathotypes coexistence frequencies with three resistances genes

Table S3 Sensitivity indices for the relative damage obtained with optimal uniform pyramiding (PyS*) and optimal uniform mosaic (MoS*) strategies for the deployment of two and three resistance genes

Notes S1 General model formulation with $nc \geq 2$ monogenic cultivars.

Notes S2 Derivation of the mutation-selection balance matrix.

Please note: Wiley Blackwell are not responsible for the content or functionality of any Supporting Information supplied by the authors. Any queries (other than missing material) should be directed to the *New Phytologist* Central Office.